Polymer Chemistry

ROYAL SOCIETY OF CHEMISTRY

PAPER

View Article Online
View Journal

Cite this: DOI: 10.1039/d6py00370b

A complementary DSC–NMR methodology for elucidating isocyanurate formation pathways in polyurethanes

Ashok Ramakrishnan, [a] Tobias Wagener,[b] Oliver Welz, [c] Berend Eling [a] and Željko Tomović *[a]

Polyurethanes (PU) are a versatile class of polymers whose properties can be tuned through chemical composition and network structure. Among these materials, rigid PU foams, formed from polyols and isocyanates in the presence of blowing agents, are widely used in construction and refrigeration applications due to their excellent insulating properties. Their fire resistance is enhanced through incorporation of isocyanurate linkages formed *via* cyclotrimerization of excess isocyanate catalyzed by potassium carboxylates, yielding polyisocyanurate (PIR) foams. A detailed understanding of the reaction sequence and associated heat release during PIR formation is essential for optimizing foam performance. Herein, we present an integrated approach combining differential scanning calorimetry (DSC) with nuclear magnetic resonance (NMR) to correlate enthalpic changes with reaction progress during isocyanurate formation. By quenching reactions at selected temperatures and analyzing mixtures by NMR, we constructed a detailed reaction profile for a mono-functional, low-molar-mass model isocyanate-alcohol system catalyzed by potassium acetate (KOAc) and potassium 2-ethylhexanoate (K-2-EH). Rapid carbamate formation occurs at low temperatures, followed by allophanate and isocyanurate formation. Allophanate acts as a key intermediate in the formation of isocyanurate till ~70 °C, above which it undergoes catalytic degradation to yield isocyanurate and carbamate. Two exothermic events observed in DSC coincided with changes in the reaction mechanism: first at 60–70 °C, arising from allophanate accumulation and concurrent isocyanurate formation; second at 80 °C, from catalytic allophanate degradation. We envisage that the combined DSC–NMR approach can provide a practical platform for studying polymer-forming systems under bulk conditions, providing insights into reaction and catalysis mechanisms.

Received 14th April 2026,
Accepted 9th May 2026

DOI: 10.1039/d6py00370b

rsc.li/polymers

1. Introduction

Polyurethanes (PU) constitute one of the most versatile classes of polymeric materials, offering a wide range of chemical, thermal, and mechanical properties through variations in molecular composition, network, and processing. This versatility has enabled their development into diverse material forms, including elastomers, coatings, adhesives, and cellular foams. Within this family, rigid PU foams constitute an important class of materials characterized by high strength-to-weight ratios and excellent thermal insulation properties, making them widely used in applications such as insulation panels for the building industry and appliances including refrigerators, freezers, and boilers. These foams are highly cross-linked, closed-cell materials produced by reacting a polyether or polyester polyol blend containing additives such as a catalyst, blowing agent, and surfactant with a polyisocyanate.[1–5] When isocyanate is used in excess relative to the amount required to react with the hydroxyl groups of the polyol component, the surplus isocyanate can be trimerized in the presence of catalysts to isocyanurate.[6] Foams produced under these conditions are referred to as polyisocyanurate (PIR) foams and are typically produced with a three to five-fold molar excess of isocyanate, corresponding to an isocyanate index of 300–500.[1,7–9] Isocyanurate shows high thermal stability, and its formation can, in practice, be considered irreversible. Moreover in polymers, it forms a stable crosslink, and consequently, polyurethanes containing isocyanurate crosslinks exhibit improved thermal resistance and reduced flammability.[10–12] The polyol segments, incorporated *via* urethane (carbamate) linkages, provide flexibility and reduce material friability.[13–15]

The production of PIR foam is more complex than that of conventional PU foams, because the carbamate and isocyanurate reactions that take place must be balanced during foam

[a]*Polymer Performance Materials Group, Department of Chemical Engineering and Chemistry, Eindhoven University of Technology, 5600 MB Eindhoven, The Netherlands. E-mail: z.tomovic@tue.nl*
[b]*BASF Polyurethanes GmbH, Elastogranstr 60, 49448 Lemfoerde, Germany*
[c]*BASF SE, Carl-Bosch-Strasse 38, 67056 Ludwigshafen, Germany*

expansion. Since the reactions are catalyst-driven, catalyst selection is critical to achieving the desired processing characteristics and mechanical properties of the produced foams. Carboxylate-based catalysts, notably potassium acetate and potassium 2-ethylhexanoate, are commonly used for isocyanurate formation in the commercial production of PIR foam.[1,15–18]

Despite the high technical and commercial importance of PIR foam in industry, the mechanism of isocyanurate formation and the role of carboxylate catalysts during the reaction remain a matter of debate, with several proposed mechanistic pathways. Broadly, we categorize the pathways leading to isocyanurate formation, based on the reacting species involved, into two groups: (i) direct trimerization and (ii) the allophanate pathway. Direct trimerization involves only isocyanate as the reactant and is generally understood to proceed *via* the 'classical anionic' catalyst-mediated mechanism (Scheme 1a).[17,19] According to this mechanism, the catalyst undergoes nucleophilic addition to an isocyanate, generating an initial intermediate, which then reacts with two additional isocyanate molecules. The polyamide chain with a degree of polymerization of 3 cyclizes to form the isocyanurate ring while releasing the catalyst. When carboxylates are used as catalysts, several anionic cycles have been proposed in the literature, differing in the identity of the active nucleophilic species. Beyond the carboxylate anion itself, recent studies show that more nucleophilic catalytic species, such as 'deprotonated amide'[20,21] or 'deprotonated urea'[21] derived from the carboxylate, may be generated during the reaction. Scheme 1a illustrates the 'classical anionic mechanism' for the direct trimerization of isocyanates and the proposed nucleophilic catalyst-containing structures when acetate is used as a catalyst.

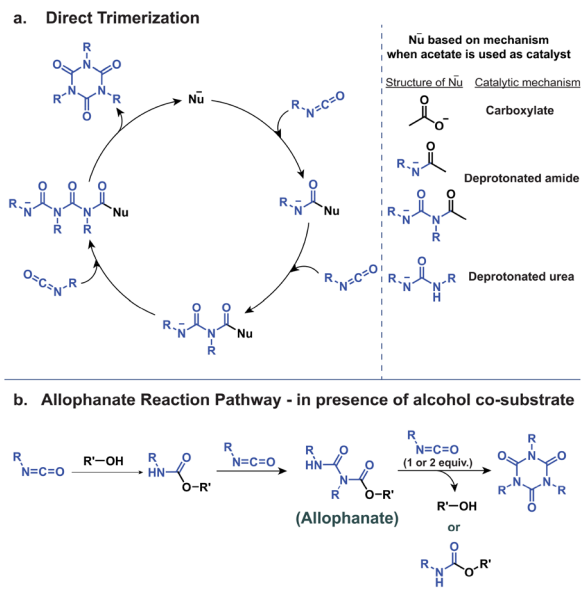

Scheme 1 (a) Direct cyclotrimerization of isocyanates *via* the generally accepted anionic mechanism. Representative structures of the active nucleophilic catalytic species – carboxylate, deprotonated amide and deprotonated urea – are shown, with acetate used as a model example.[20,21] (b) Cyclotrimerization of isocyanates in the presence of alcohol co-substrate *via* the allophanate pathway.[28]

In the presence of hydroxyl-containing co-substrates, generally in the form of polyols, isocyanurate formation may proceed *via* the 'allophanate pathway' (Scheme 1b).[17,22–28] Here, an allophanate intermediate is produced by reaction of a carbamate with an isocyanate, which subsequently reacts with additional isocyanate(s) to yield isocyanurate, thereby releasing either an alcohol or a carbamate.

Although the chemistry of catalytic direct trimerization of isocyanates in the presence of carboxylates is well documented,[17] detailed information on the reaction pathways in systems containing isocyanates and hydroxyl groups remains scarce. This is largely due to the inherent complexity of the chemistry involving various reaction pathways and numerous chemical intermediates.[18,25,26] The challenge in elucidating these pathways arises not only from the complexity of the analytical data but also from the difficulty of directly correlating the conditions of the model reactions used for mechanistic studies with those of bulk polymerizations that form foams. Several studies on the trimerization of isocyanates employ solvents that can significantly influence the reaction course.[26–29] In addition, reaction time, temperature, catalyst choice, and the isocyanate-to-hydroxyl group ratio can influence the mechanistic interpretation, further complicating the mechanistic understanding of these systems.

To address these challenges, we developed a new methodology to investigate the isocyanate cyclotrimerization reaction pathway using a low-molar-mass, monofunctional model system designed to closely mimic bulk PIR formulations. Herein, we report a study of the reaction between an alcohol and an excess of isocyanate catalyzed by potassium carboxylates, employing both 'Differential Scanning Calorimetry' (DSC) and 'Nuclear Magnetic Resonance' (NMR) spectroscopy. DSC allows approximation of the temperature conditions experienced during pseudo-adiabatic foam formation by applying a controlled heating ramp. Quenching reactions at selected points along the resulting DSC exotherm and analyzing the mixtures by NMR enable the determination of the compositions of reactants, intermediates, and products at successive stages, thereby providing a framework for elucidating the reaction pathways involved in isocyanurate formation. The reactions were performed in the absence of solvents, and industry-relevant catalysts were employed.

2. Results and discussion

2.1. Model reaction

The cross-linked network in conventional PIR foams is formed by reactions between polyisocyanates, such as poly(methylene diphenyl diisocyanate) (pMDI), and polyols. Commercial PIR formulations typically employ an isocyanate index exceeding 300.[1,2,9,30] Under these conditions, multiple competing reactions may occur, leading to the formation of (a) carbamate lin-

kages *via* equimolar isocyanate-alcohol addition, (b) allophanate linkages through the equimolar reaction of isocyanate with carbamate, and (c) isocyanurate structures arising from trimerization reactions of isocyanates.

To probe the pathways leading to isocyanurate formation while minimizing system complexity, a model reaction using monofunctional analogues of the isocyanate and hydroxyl components was employed. The geometry and electronic structures of their reactive groups closely resemble those of the polyfunctional reactants in real foaming systems, namely pMDI and polyether polyols. The low molar masses of the reactants and products enable the use of spectroscopic techniques for a detailed analysis. The compounds, *p*-tolyl isocyanate (*p*TI) and 2-ethoxyethanol (EE) were selected as representative isocyanate and alcohol substrates, respectively, and were reacted in a 4 : 1 molar ratio. Complete conversion to isocyanurate (ISR) and carbamate (CRB) would theoretically yield these products in a 1 : 1 molar ratio. However, intermediates such as allophanate (APH) are also formed during the reaction.[25,28] Potassium acetate (KOAc) and potassium 2-ethylhexanoate (K-2-EH) were employed with a total catalyst loading fixed at 0.375 mol% relative to isocyanate groups. A general scheme of the reactants and expected products is provided in Scheme 2.

2.2. Methodology to study the reaction pathway

PU foams are formed under pseudo-adiabatic conditions. To mimic the exotherm of a foaming reaction, we employed DSC to apply a linear temperature ramp to our model reaction over the relevant temperature range. The exotherms observed during the temperature scan are associated with the enthalpy changes accompanying the chemical transformations. Prior to the reaction, the catalysts were dissolved in EE, and the samples were prepared by mixing the required amounts of *p*TI with EE containing the catalyst. A small portion of the resulting mixture was then transferred into a DSC pan, sealed with a lid, and loaded into the instrument for DSC analysis. The entire sample preparation and loading process required approximately 5 min. The sample was heated at 10 °C min^{-1} from 25 to 120 °C, revealing its overall exothermic behavior. Upon completion of the reaction, the sample was cooled to 25 °C and removed from the instrument. The DSC pan was carefully opened, and the reaction mixture was chemically quenched with thionyl chloride (dissolved in $CDCl_3$) to deactivate the catalyst. NMR analysis of the fully reacted mixture confirmed quantitative formation of isocyanurate (ISR) and carbamate (CRB) in a 1 : 1 molar ratio (Tables S1 and S2, SI).

To gain insight into the reaction progression, independent reactions were run and stopped at predefined temperatures, corresponding to specific thermal events observed in the complete DSC scans. Each partially reacted sample was quenched as described above and analyzed by NMR spectroscopy to determine the composition of reactants, intermediates, and products at that stage. Correlation of these compositions across multiple temperature points enabled the construction of a 'reaction composition profile' depicting the changes in composition of each species as a function of temperature, providing insight into the operative mechanistic pathway. The overall workflow of the study is illustrated in Fig. 1. Detailed experimental procedures for studying the reaction pathway using DSC and NMR analyses are provided in Section S2 of the SI.

2.3. DSC exotherms of model reaction using KOAc and K-2-EH as catalysts

The full DSC scans for the reactions catalyzed by KOAc and K-2-EH are shown in Fig. 2a. The overall exothermic behavior of the two scans was similar, with two distinct exothermic events observed in each case. For KOAc, the first exotherm began to rise at approximately 50 °C and reached its first maximum at about 70–75 °C (T_1). After reaching this maximum, the heat flux decreases sharply, then increases again, resulting in a sharp second maximum at approximately 80 °C (T_2). Thereafter, the heat flux then gradually decreases again and returns to the baseline at approximately 100–110 °C, indicating completion of the reaction.

The DSC profile obtained with K-2-EH followed a similar trend, with notable differences in the onset and maximum of the first exotherm. In this case, the initial exothermic event began at approximately 40 °C and peaked at approximately 60 °C (T_1). The second maximum (T_2) and reaction completion occurred at temperatures comparable to those observed for the KOAc-catalyzed system. As in the KOAc case, the final reaction mixture consisted of equimolar amounts of isocyanurate (ISR) and carbamate (CRB).

2.4. Reaction profile of KOAc and K-2-EH catalyzed reactions

Guided by the full DSC scans, multiple reactions of the model system were conducted up to predetermined temperatures.

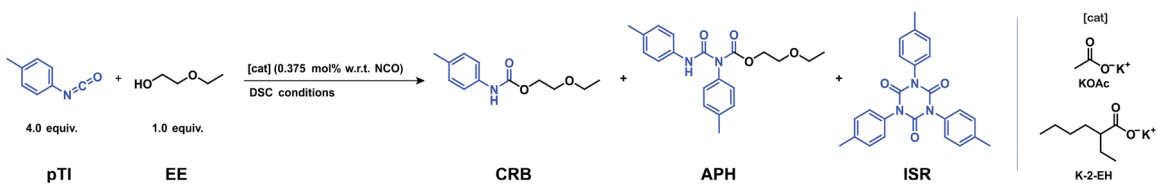

Scheme 2 Model reaction depicting the reactants used and all the expected intermediates and products considered for this study. Reactants: *p*-tolyl isocyanate (*p*TI, 4.0 equiv.) and ethoxyethanol (EE, 1.0 equiv.), products: carbamate (CRB), allophanate (APH) and isocyanurate (ISR); catalyst concentration used is 0.375 mol% relative to *p*TI. The catalysts employed in this study were potassium acetate (KOAc) and potassium 2-ethylhexanoate (K-2-EH).

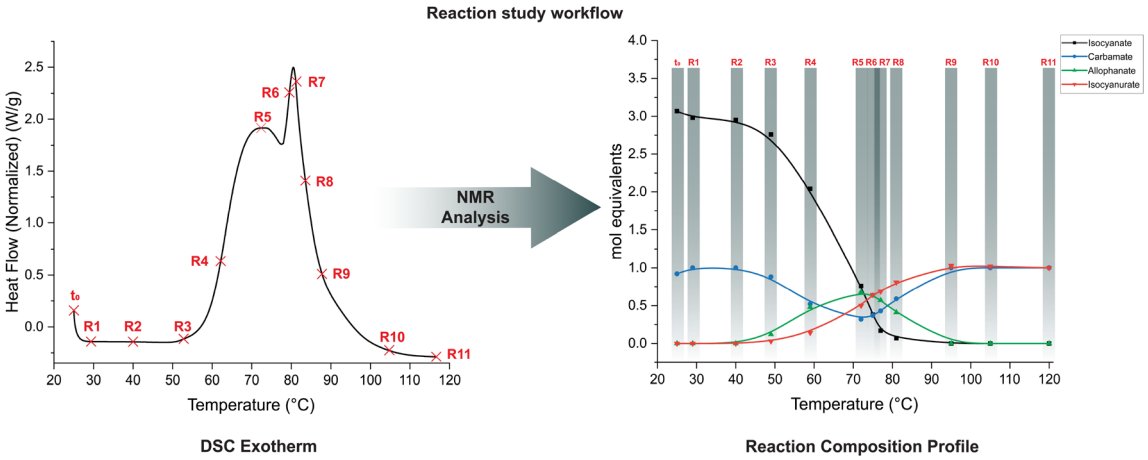

Fig. 1 Mapping of the reaction pathway of the model system by plotting reaction composition against temperature. Each run (R1–R11) represents an independent DSC experiment, with the corresponding sample analyzed by NMR to determine its composition.

The resulting mixtures were quenched and analyzed by ^{1}H NMR. Changes in ^{1}H NMR spectra arising from variation in reaction mixture composition, along with the corresponding reaction composition profiles for the KOAc and K-2-EH catalyzed reactions, are provided in Fig. 2b and c. The detailed analysis of the individual runs is presented in Tables S1 and S2 of the SI.

Analysis of the concentrations of the products – carbamate (CRB), formed by equimolar reaction of *p*TI and EE, allophanate (APH), formed by equimolar reaction of CRB with *p*TI, and isocyanurate (ISR), formed *via* direct or allophanate-mediated cyclotrimerization – at each stage enables identification of the dominant reactions as a function of temperature. For clarity, the reaction composition profiles are divided into three phases based on the allophanate (APH) profile.

2.4.1. Phase I (onset of APH formation). At the start of the measurement at 25 °C, ^{1}H NMR analysis revealed that CRB formation was already largely complete, reaching 92% and 96% relative to the alcohol substrate EE for the KOAc and K-2-EH-catalyzed reactions, respectively. This shows that potassium carboxylates effectively catalyze the formation of carbamate. Consequently, the full DSC scan shows negligible heat release associated with carbamate formation. Analysis of the reaction composition at the onset of the first exothermic peak in the DSC scans in both reactions coincides with the initiation of APH formation.

2.4.2. Phase II (accumulation of APH). During this phase, rapid consumption of *p*TI and CRB occurred, accompanied by increased APH and ISR formation. At T_1, APH reached a maximum value of ~0.7 mol equivalent, corresponding to approximately 70% of the originally available CRB. At T_1, *p*TI and APH were present in roughly equimolar amounts.

2.4.3. Phase III (decline of APH). Beyond T_1, the amount of APH decreased. This was accompanied by a drop in *p*TI below the APH level; between T_1 and T_2, the amount of *p*TI fell to less than 0.2 mol equivalent, significantly lower than that of APH (~0.2 to 0.6 mol equivalent). The second exotherm was characterized by a sudden increase in heat flow, peaking at T_2. The exotherm ended with complete conversion to ISR and CRB, with an ISR : CRB molar ratio of 1 : 1.

2.5. DSC studies on APH

APH undergoes thermal degradation above 150 °C.[31,32] This was confirmed by TGA analysis of a synthesized pure APH model compound: the onset of degradation occurred at 146 °C, and 5 wt% loss was observed at 165 °C (Fig. S3, SI). The stability of APH under the present dynamic reaction conditions was studied by DSC, scanning from 25 to 120 °C in the presence and absence of catalyst, and additional isocyanate (Fig. 3 and Table S3, SI).

In the absence of the catalyst, no exotherm was observed, and ^{1}H NMR analysis confirmed that APH, as expected, remained unreacted.

In the presence of K-2-EH, the DSC scan first shows an endothermic process that begins at 80 °C and peaks at 86 °C. Shortly thereafter, the heat flow changes over a short temperature interval from endo to exo, with the exothermic process peaking at 91 °C. The endothermic process is ascribed to the degradation of APH into CRB and *p*TI, whereas the exothermic reaction represents the conversion of *p*TI to ISR. ^{1}H NMR analysis of the reaction mixture at the end of the DSC scan indeed confirmed complete conversion of APH to ISR and CRB (Fig. S4 and Table S3, SI).

Upon addition of an equimolar amount of *p*TI and catalytic amounts of K-2-EH to APH, the reaction started readily. Even after 5 minutes at room temperature, some ISR and CRB had formed, with ISR exceeding CRB (Fig. S5, SI). The formed CRB likely resulted from APH degradation, and the initial formation of ISR from the direct trimerization of *p*TI promoted by the relatively high catalyst loading. The corresponding DSC scan exhibited features similar to those of the model reaction between *p*TI and EE, with the first exotherm peaking at 60 °C (T_1) and the second at approximately 80 °C (T_2). This reaction

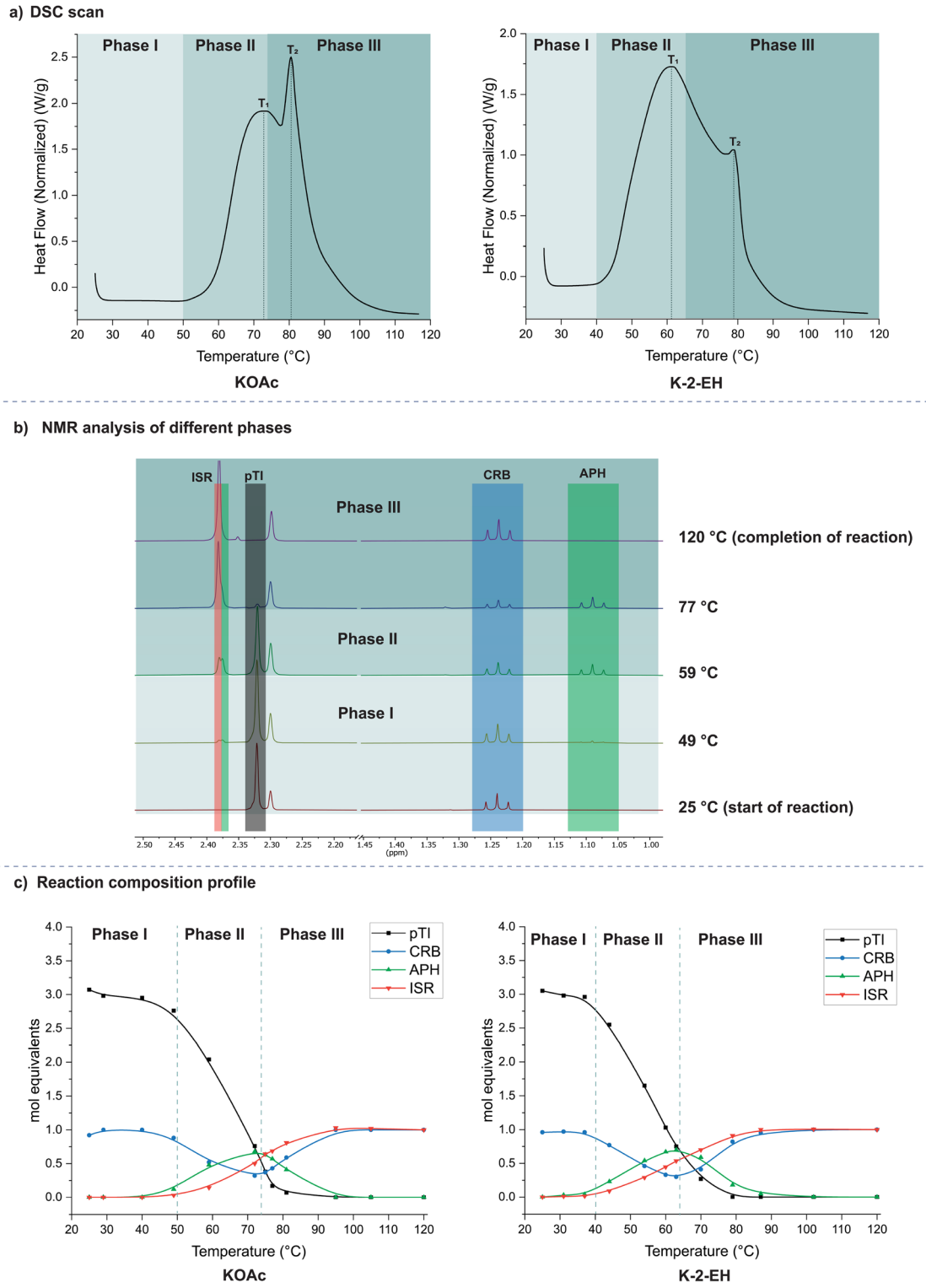

Fig. 2 (a) DSC scans of the model reaction catalyzed by KOAc and K-2-EH, highlighting the distinct phases of the reaction. (b) Representative ^{1}H NMR spectra in the chemical shift region of 1.0 to 2.5 ppm, highlighting compositional changes across the phases; spectra shown for KOAc. K-2-EH exhibits a similar trend. (c) Reaction composition profile depicting the phases of the model reaction catalyzed by KOAc and K-2-EH. Reaction: *p*TI (4.0 equiv.), EE (1.0 equiv.), catalyst (0.375 mol% relative to NCO). DSC conditions: temperature range set as 25 to 120 °C, heating ramp set at 10 °C min^{-1}. The error associated with sampling at the DSC temperature is estimated to be ±2.5 °C.

also proceeded to completion, yielding ISR and CRB as the final products (Fig. S6, SI).

It is important to note that the catalytic degradation of APH is strongly influenced by the choice of (NMR) solvent used for analysis at the end of the reaction. For instance, DMSO-d_6 markedly accelerates the catalytic degradation of APH, whereas $CDCl_3$ has little effect (Section S4.5, Fig. S9 and S10, SI). This also highlights the significant impact of solvents on these reactions and indicates that observations made in model systems containing solvent may differ from those performed under solvent-free or bulk conditions.

2.6. Reaction pathway

The reaction composition profile (Fig. 2c) reflects the sequence of chemical events occurring in the temperature scan. Formation of CRB from EE and -*p*TI occurred almost instantaneously (relative to the time scale of the sample preparation) and was largely complete by the time the DSC measurement began. Consequently, the composition at the start of the scan consisted of ~3.0 equivalents of *p*TI and ~1.0 equivalent of CRB. As the reaction progressed, APH formation was initiated by equimolar reaction of CRB with *p*TI. In parallel, ISR formation was observed. ISR may have been formed either through 'direct trimerization of isocyanates' or 'via the allophanate pathway'. APH reached a maximum, at which point the molar amounts of *p*TI and APH were comparable. Beyond this stage, APH started to decline, accompanied by increases in CRB and ISR. Notably, the consumption rate of *p*TI exceeded that of APH, indicating a stoichiometric deviation required for the allophanate–isocyanate reaction pathway. In addition, the formation of ISR *via* direct trimerization reaction alone is limited due to the low availability of *p*TI. Following near-complete depletion of *p*TI, APH degradation was the sole potential source of *p*TI for ISR formation, thereby leading to CRB formation. Consequently, 'catalytic degradation of allophanate' becomes the dominant pathway in the later stages of the reaction to form ISR. This is consistent with the widely accepted view that allophanates function as isocyanate reservoirs,[31] from which the catalyst-induced release of isocyanate enables subsequent isocyanurate formation. The endothermic feature observed in the DSC trace during the degradation of APH in the presence of a catalyst may therefore be associated with isocyanate release from APH (Fig. 3).

The degradation of allophanate at low isocyanate concentrations was also observed by Špírková *et al.* during the reaction between phenyl isocyanate and butanol under isothermal conditions.[26] In their study, the formation of urea, alongside carbamate, was attributed to the reaction of water with allophanate, which released alcohol and carbon dioxide. However, the present work suggests that these products may have formed instead from the reaction of water, present in the solvent, with isocyanate released during catalytic allophanate degradation.

Linking these reaction events with the DSC exotherm phases enabled us to assign which parts of the exotherm correspond to which reaction stage. The first exothermic event, corresponding to Phase II of the DSC profile, was associated with the formation and accumulation of APH, occurring in parallel with the formation of ISR. The maximum of the first exotherm coincided with the maximum in APH. Thereafter, the amount of *p*TI fell below that of APH, and the dominant ISR forming pathway shifted to 'catalytic allophanate degradation followed by isocyanurate and carbamate formation'. The latter defines Phase III of the reaction profile, during which ISR is produced with concurrent CRB formation. This transition coincided with the appearance of the second exothermic event in Phase III of the DSC scan. A summary of

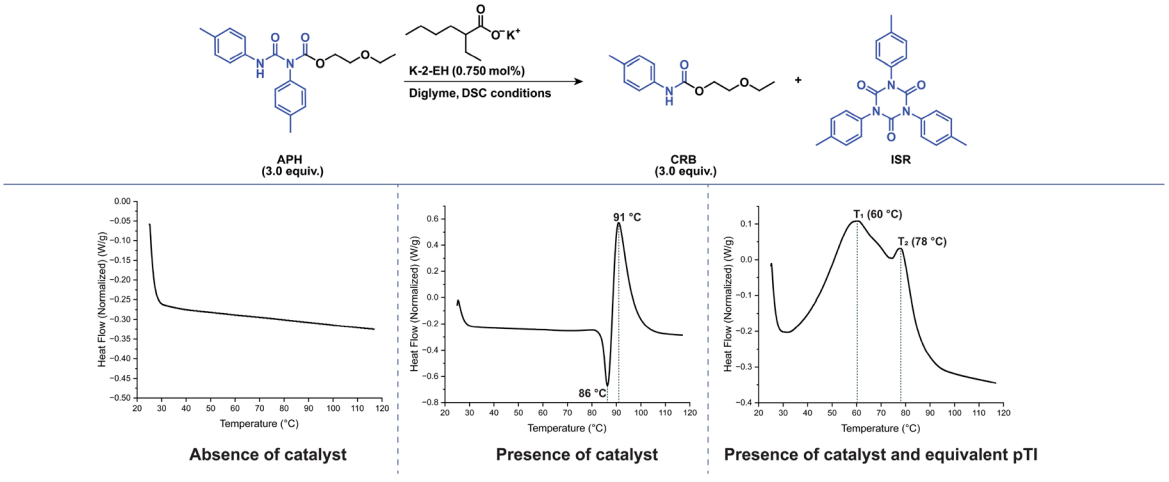

Fig. 3 DSC scans of APH catalytic degradation under three conditions: (i) in the absence of catalyst, (ii) in the presence of K-2-EH, and (iii) in the presence of K-2-EH with an equimolar amount of *p*TI. Catalytic reaction conditions (ii): APH (20 mg, 56.1 μmol), K-2-EH (0.750 mol% relative to APH, 0.4 μmol, 76.7 μg), diglyme (20 μL). Absence of catalyst (i): No K-2-EH was used. Presence of catalyst and equivalent of *p*TI (iii): K-2-EH (1.125 mol% relative to APH or 0.375 mol% relative to NCO/NCO derived molecules, 0.6 μmol, 112.5 μg), *p*TI (7.5 mg). DSC conditions: Temperature range 25–120 °C, heating ramp: 10 °C min^{-1}.

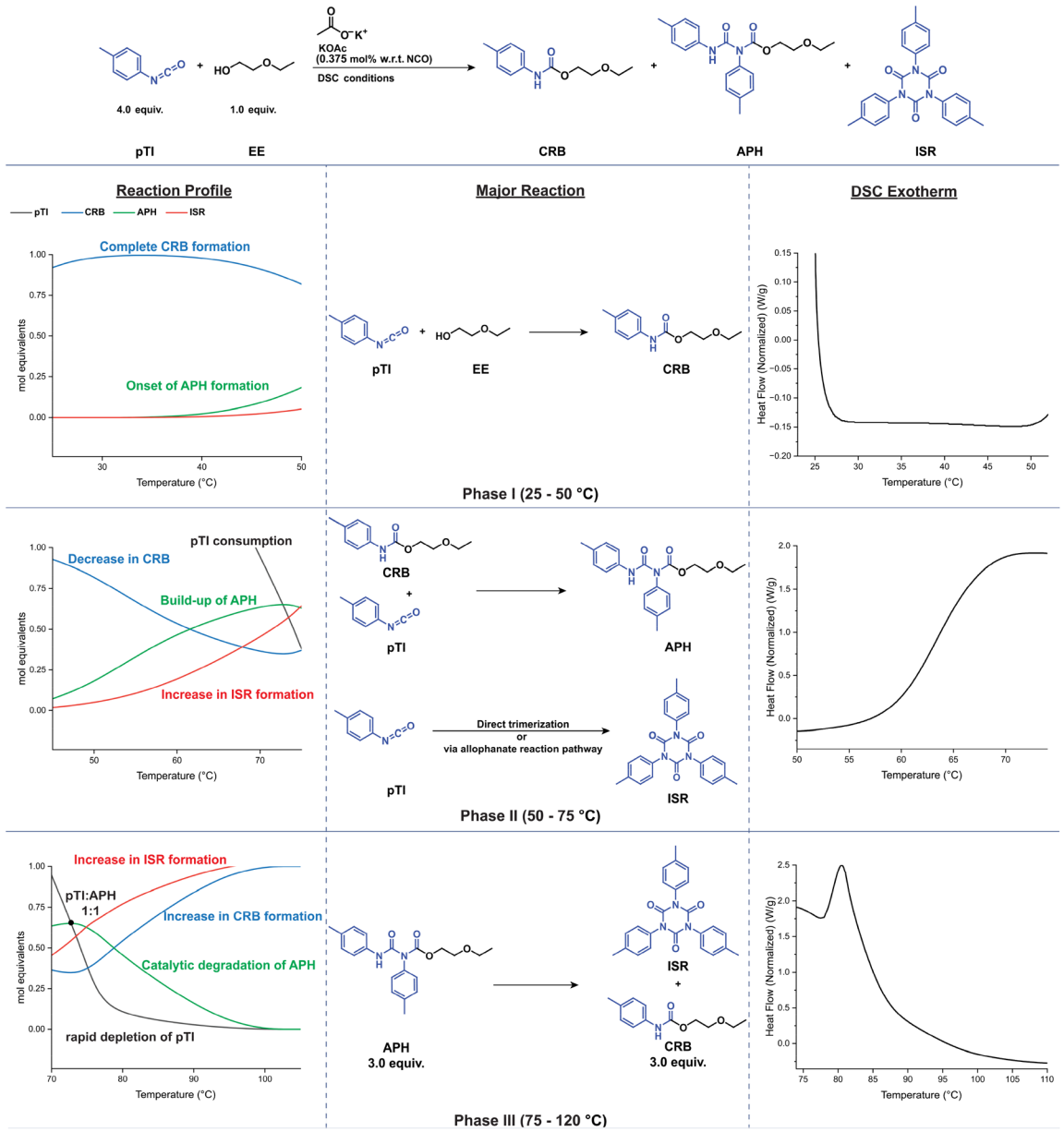

Fig. 4 Reaction profile, major reactions occurring at the various stages, and DSC exotherm clippings corresponding to each phase of the model reaction catalyzed by KOAc. Reaction conditions: *p*TI (4.0 equiv.), EE (1.0 equiv.), KOAc (0.375 mol% relative to NCO). DSC conditions: temperature range set as 25 to 120 °C, heating ramp set at 10 °C min^{-1}, error associated with the recording rate of the DSC exotherm is estimated to be ±2.5 °C.

the reaction sequence for the KOAc-catalyzed model system is shown in Fig. 4.

The differences observed in the DSC profiles for the KOAc- and K-2-EH-catalyzed reactions may arise from variations in anion nucleophilicity as well as from differences in the solubility of the carboxylate salts in the reaction medium. Ethylhexanoate, being more nucleophilic than acetate, can promote earlier initiation of the reaction. In addition, KOAc is likely less soluble in the relatively apolar environment, limiting the initial availability of acetate in the organic phase. As the reaction progresses, however, acetate is increasingly transferred into the liquid phase *via* ongoing chemical transformations, thereby becoming catalytically active. In contrast, K-2-EH is better solubilized from the outset of the DSC experiment due to its superior compatibility with the reaction medium, ensuring earlier catalytic availability. As a result, T_1 of KOAc is shifted to higher temperatures than T_1 of K-2-EH. The chemistry underlying the second peak, however, occurs in a similar temperature range for both catalysts. Because T_1 occurs at a higher temperature in the KOAc-catalyzed reaction, the second peak is elevated and thus becomes more pronounced. Near T_2, catalytic degradation of allophanate is particularly evident. The sudden release of isocyanate increases the formation rate of ISR, as indicated by a higher heat flux.

The experimental enthalpies associated with isocyanurate formation, derived from the full DSC scans for KOAc and K-2-EH, are 124 and 122 kJ mol^{-1}, respectively. Since carbamate formation is already complete before the DSC run begins and the final product is isocyanurate, the measured exotherm can be attributed primarily to the enthalpy of isocyanurate formation. This corresponds to a reaction enthalpy of 40 kJ mol^{-1} per isocyanate, approximately half that of carbamate formation.[33]

3. Conclusions

We developed a novel integrated DSC–NMR approach to elucidate the reaction pathway in polyisocyanurate (PIR) formulations. Application of this methodology to a model system employing mono-functional substrates and potassium carboxylates as catalysts enabled mapping of the reaction sequences and associated heat flow.

The carbamate reaction occurs first; it proceeds rapidly at low temperatures and is completed before subsequent reactions start. After completion of the carbamate reaction, allophanate and isocyanurate are formed. Isocyanurate can be formed by either a direct catalyst-mediated reaction of isocyanate or *via* a catalytic route in which allophanate is formed as a chemical intermediate – the 'direct' and 'allophanate mediated' trimerization route. The amount of isocyanurate increases continuously, whereas allophanate reaches a maximum at approximately 60 °C and then declines primarily due to catalytic degradation, forming carbamate and isocyanurate – the final products of the reaction. The reaction accelerates when the catalytic degradation of allophanate and subsequent conversion to isocyanurate begin, occurring after depletion of the isocyanate reactant, resulting in a sudden increase in heat release rate at 80 °C.

We envision that this approach will be broadly applicable to the study of reaction mechanisms in other established resin systems, providing mechanistic insight into reaction pathways and corresponding heat-flow profiles. Moreover, the methodology provides a powerful platform for investigating catalyst performance and reaction behavior, thereby aiding the rational design and development of improved resin systems.

Conflicts of interest

There are no conflicts to declare.

Data availability

Supplementary information (SI): experimental procedure details, DSC–NMR experimental data, characterization data. See DOI: https://doi.org/10.1039/d6py00370b.

Acknowledgements

The authors acknowledge financial support from BASF Polyurethanes GmbH.

References

1 B. Eling and W. Friederichs, *Polyurethanes: Polyols, Isocyanates, Rigid Foams, Flexible Foams*, Elastomers, De Gruyter, 2025, pp. 125–158.
2 K. Dedecker, J. Deschaght and M. Barker, in *The Polyurethanes Book*, ed. S. Lee and D. Randall, J. Wiley, 2002, pp. 229–271.
3 B. Eling, Ž Tomović and V. Schädler, *Macromol. Chem. Phys.*, 2020, **221**, 2000114.
4 H.-W. Engels, H.-G. Pirkl, R. Albers, R. W. Albach, J. Krause, A. Hoffmann, H. Casselmann and J. Dormish, *Angew. Chem., Int. Ed.*, 2013, **52**, 9422–9441.
5 R. K. Traeger, *J. Cell. Plast.*, 1967, **3**, 405–418.
6 E. Delebecq, J.-P. Pascault, B. Boutevin and F. Ganachaud, *Chem. Rev.*, 2013, **113**, 80–118.
7 D. A. Hicks, M. C. Barker, A. L. R. M. P. Herssens and M. L. Green, WO2000017248A1, 2000.
8 H. Verbeke and A. A. Vanhalle, WO2015150408A1, 2015.
9 L. Pellacani, P. Golini and P. Keller, WO2012083038A1, 2012.
10 Y. Guo, J. Kleemann, S. Bokern, A. Kamm, R. P. Sijbesma and Ž Tomović, *Polym. Chem.*, 2023, **14**, 1923–1932.
11 Y. Guo, J. Kleemann, R. P. Sijbesma and Ž Tomović, *ACS Appl. Polym. Mater.*, 2023, **5**, 4689–4697.
12 C. Wang, Y. Guo, T. Türel and Ž Tomović, *ACS Appl. Mater. Interfaces*, 2024, **16**, 35604–35612.
13 E. K. Moss and D. L. Skinner, *J. Cell. Plast.*, 1976, **12**, 332–336.
14 E. K. Moss and D. L. Skinner, *J. Cell. Plast.*, 1977, **13**, 276–282.
15 D. K. Hoffman, *J. Cell. Plast.*, 1984, **20**, 129–137.
16 M. Špírková, M. Kubín, P. Špaček, I. Krakovský and K. Dušek, *J. Appl. Polym. Sci.*, 1994, **52**, 895–904.
17 Y. Guo, M. Muuronen, F. Lucas, R. P. Sijbesma and Ž Tomović, *ChemCatChem*, 2023, **15**, e202201362.
18 J. Reignier, F. Méchin and A. Sarbu, *Ind. Eng. Chem. Res.*, 2024, **63**, 20824–20839.
19 I. Bechara, *J. Cell. Plast.*, 1979, **15**, 102–113.
20 Y. Guo, M. Muuronen, P. Deglmann, F. Lucas, R. P. Sijbesma and Ž Tomović, *J. Org. Chem.*, 2021, **86**, 5651–5659.
21 M. Siebert, R. Sure, P. Deglmann, A. C. Closs, F. Lucas and O. Trapp, *J. Org. Chem.*, 2020, **85**, 8553–8562.
22 I. C. Kogon, *J. Am. Chem. Soc.*, 1956, **78**, 4911–4914.
23 I. C. Kogon, *J. Am. Chem. Soc.*, 1959, **24**, 83–86.
24 I. C. Kogon, *J. Org. Chem.*, 1961, **26**, 3004–3005.
25 M. Špirková, M. Kubín and K. Dušek, *J. Macromol. Sci., Chem.*, 1987, **A24**, 1151–1166.

26 M. Špírková, M. Kubín, P. Špaček, I. Krakovský and K. Dušek, *J. Appl. Polym. Sci.*, 1994, **53**, 1435–1446.
27 K. Schwetlick and R. Noack, *J. Chem. Soc., Perkin Trans. 2*, 1995, 395–402.
28 A. Al Nabulsi, D. Cozzula, T. Hagen, W. Leitner and T. E. Müller, *Polym. Chem.*, 2018, **9**, 4891–4899.
29 W. Wejchan-Judek, I. Polus, B. Doczekalska and H. Pertek, *Polimery*, 2001, **46**, 131–132.
30 P. Golini, WO2010114703A1, 2010.
31 G. Laqua, M. Klötzer, V. Krase, P. Pfab, J. Pfeffinger and A. Schmidt, *United States Pat*, US6750365B2, 2004.
32 V. V. Zharkov and R. R. Vlasov, *J. Cell. Plast.*, 2022, **58**, 877–891.
33 L. D. Artavia and C. W. Macosko, *Low density cellular plastics: Physical basis of behaviour*, Springer, 1994, pp. 22–55.